

## Support information

### **Anomalous thermal activating green upconversion luminescence in Yb/Er/ZnGdO self-assembled microflowers for high-sensitivity temperature detection**

Wei Zheng<sup>‡1</sup>, Aifeng He<sup>‡1</sup>, Hong Ma<sup>1</sup>, Jianhua Chen<sup>1</sup>, Bo Jing<sup>1</sup>, Yan Li<sup>1</sup>, Xiaogang Yu<sup>1</sup>, Chunqiang Cao<sup>1</sup>, Baoyu Sun<sup>1,2\*</sup>

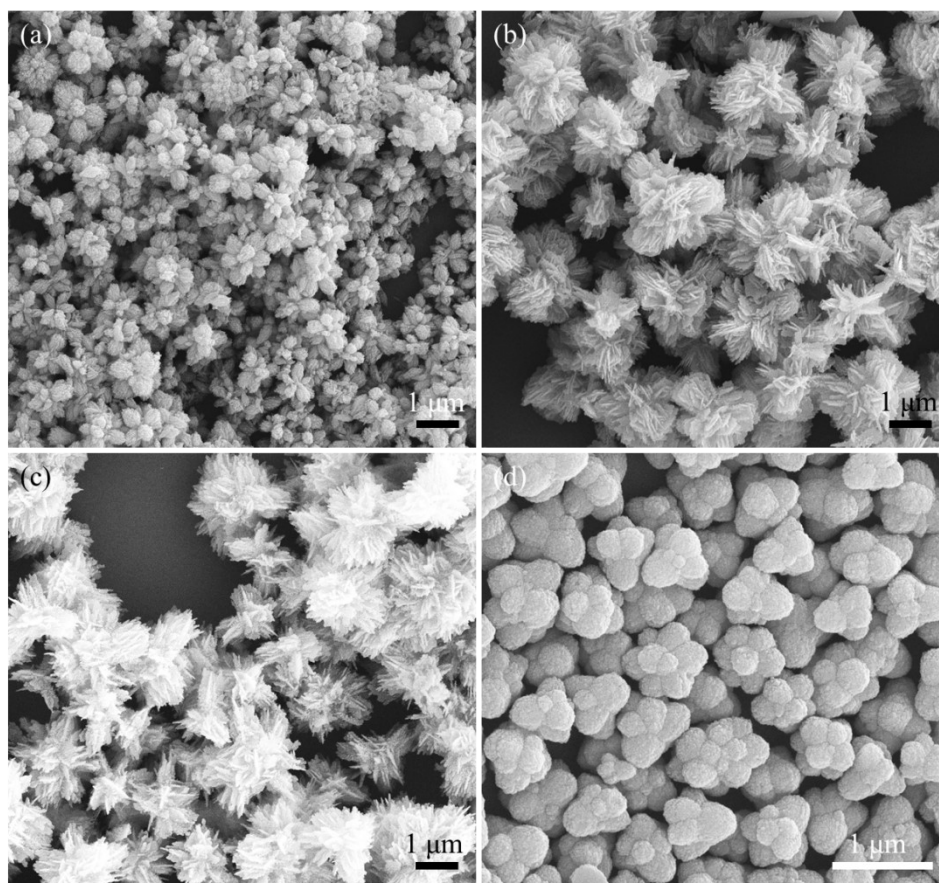
1. Key Laboratory of Applied Physics and Chemistry, Shaanxi Applied Physics and Chemistry Research Institute, Xi'an, 710061, China.

2. State Key Laboratory for Mechanical Behavior of Materials, Xi'an Jiaotong University, Xi'an 710049, China.

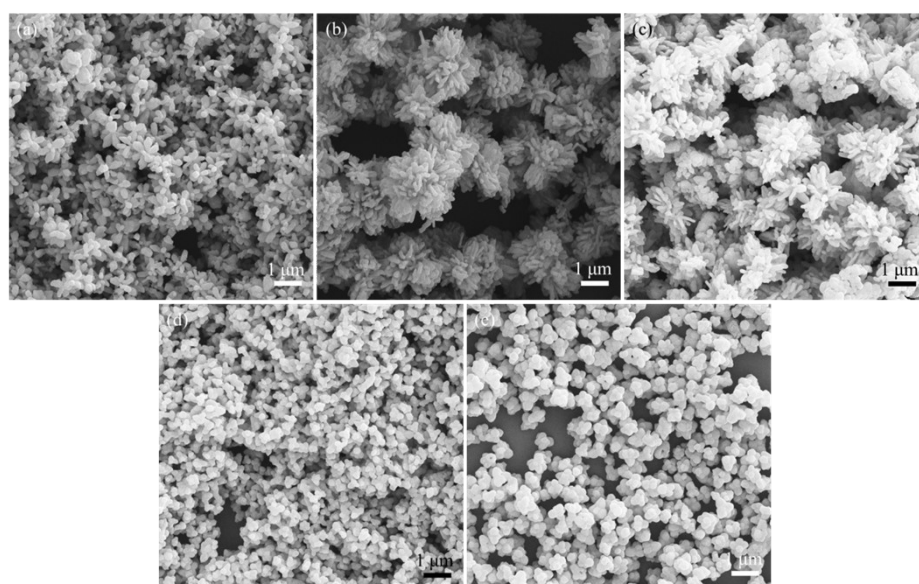
<sup>‡</sup> Equally contributed.

**Corresponding Author**

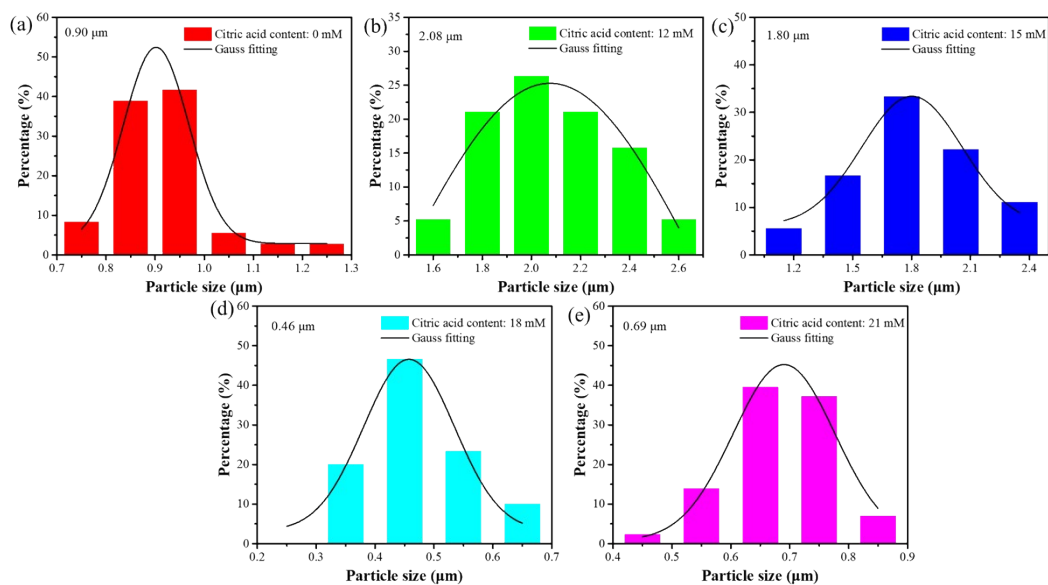
Baoyu Sun: [baoyu.sun@xjtu.edu.cn](mailto:baoyu.sun@xjtu.edu.cn)



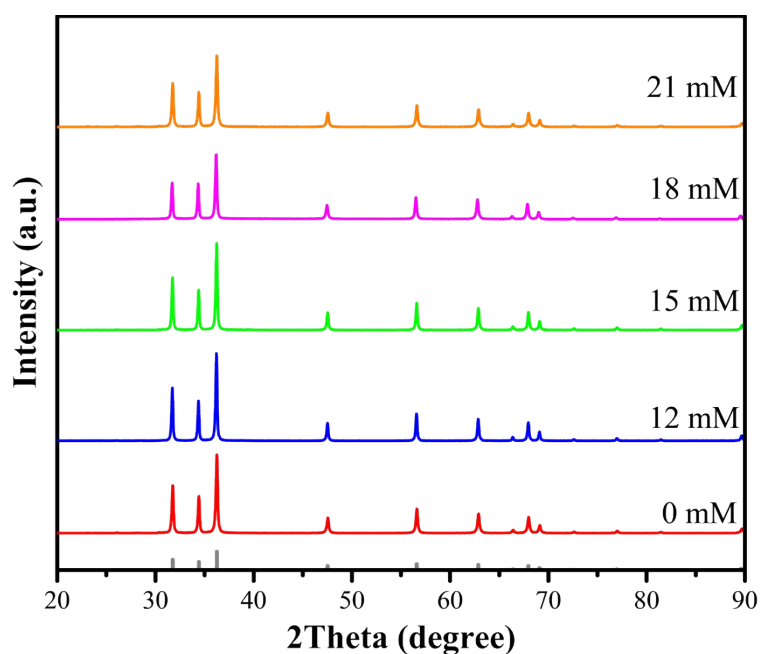
**Fig. S1.** SEM images of precursor microflowers with different citric acid content (a) 0 mM, (b) 12 mM, (c) 15 mM and (d) 21 mM.



**Fig. S2.** SEM images of Yb/Er/ZnGdO micro-flowers with citric acid content (a) 0 mM, (b) 12 mM, (c) 15 mM, (d) 18 mM and (e) 21 mM.



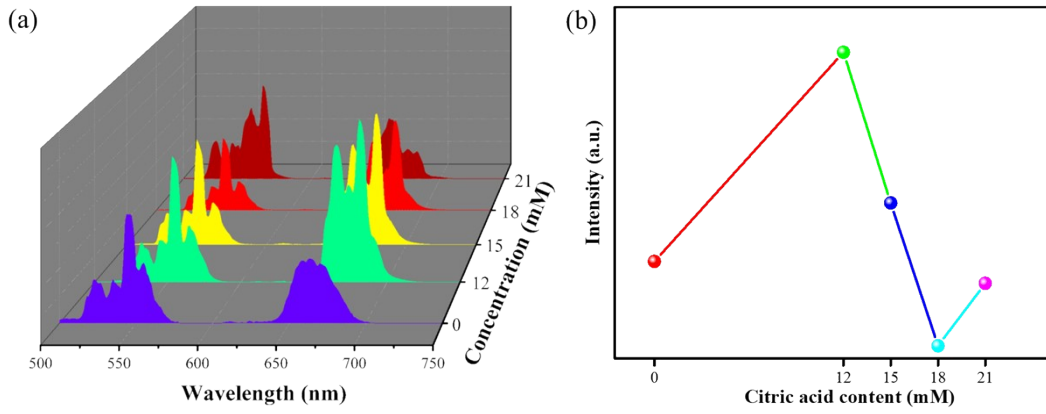
**Fig. S3.** The average diameter of Yb/Er/ZnGdO micro-flowers with citric acid content (a) 0 mM, (b) 12 mM, (c) 15 mM, (d) 18 mM and (e) 21 mM.



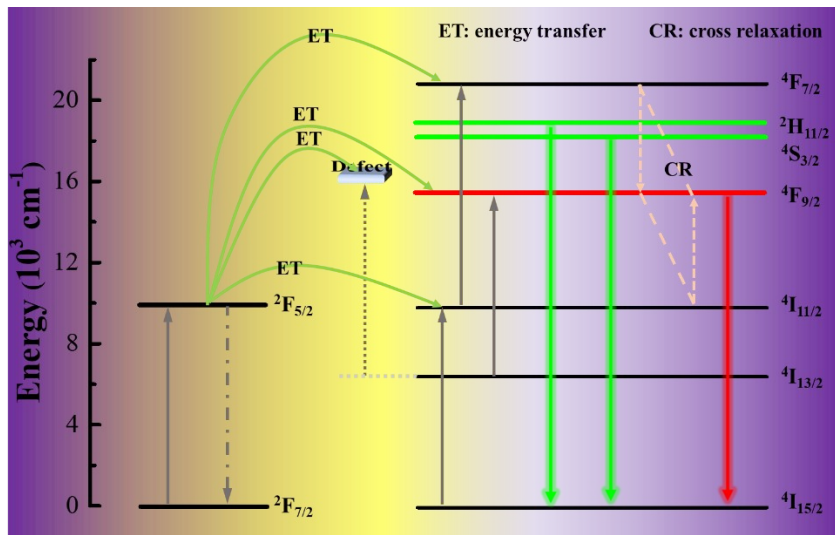
**Fig. S4.** XRD patterns of Yb/Er/ZnGdO particles with different citric acid content.

Table S1 Crystal crystallinity of Yb/Er/ZnGdO particles with different citric acid content.

Citric acid content (mM)	Crystallinity/(100) crystal planes	Crystallinity/(002) crystal planes
0	86%	76%
12	95%	96%
15	91%	92%
18	84%	69%
21	80%	66%



**Fig. S5.** (a) Upconversion luminescence spectra of Yb/Er/ZnGdO particles with different content of citric acid. (b) The variation of total emission intensity with content of citric acid.



**Fig. S6.** Proposed the upconversion emission mechanism.

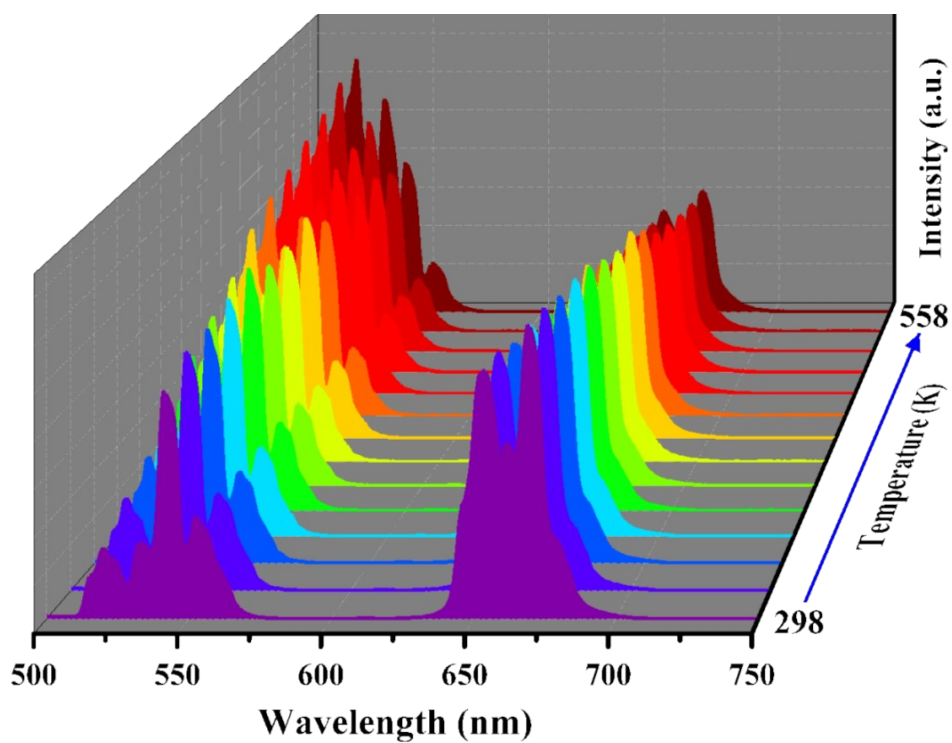


**Fig. S7.** Temperature dependent upconversion luminescence spectra of Yb/Er/ZnGdO particles with citric acid content 12 mM.

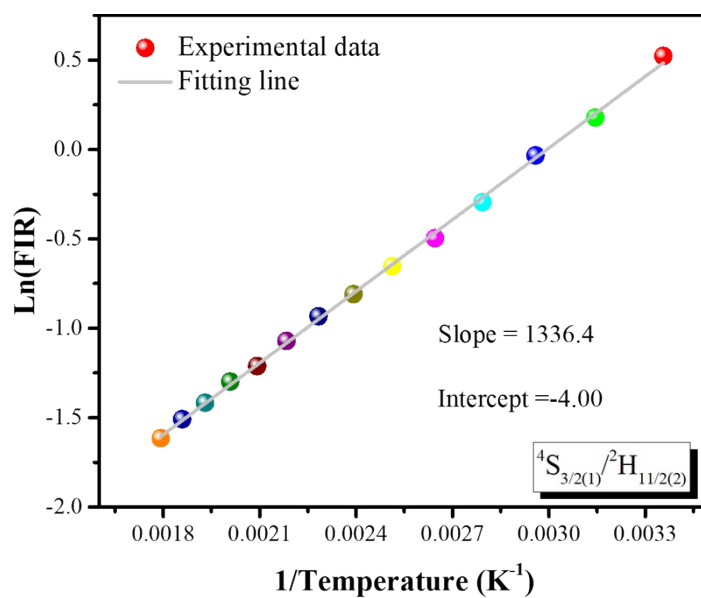


**Fig. S8.** Monolog plot of the FIR from TCL pairs based on sublevels  ${}^4S_{3/2(1)}/{}^2H_{11/2(2)}$  vs inverse absolute temperature.

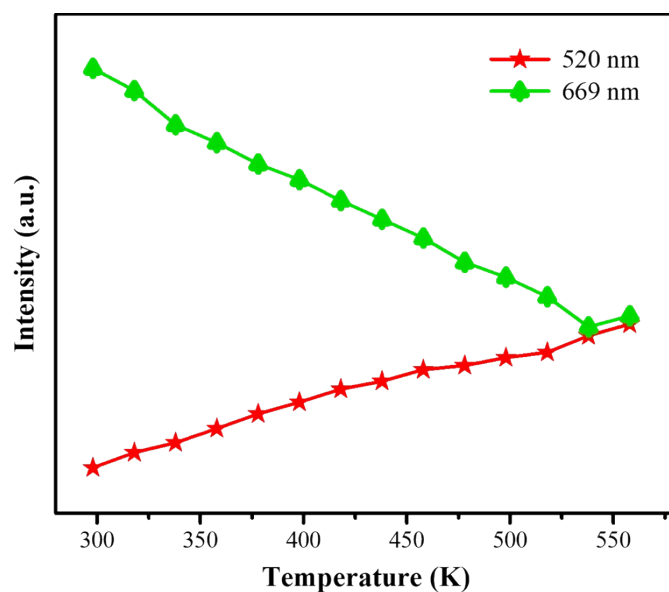


**Fig. S9.** Temperature dependent upconversion emitting intensity at 520 nm and 669 nm for Yb/Er/ZnGdO particles with citric acid content 12 mM

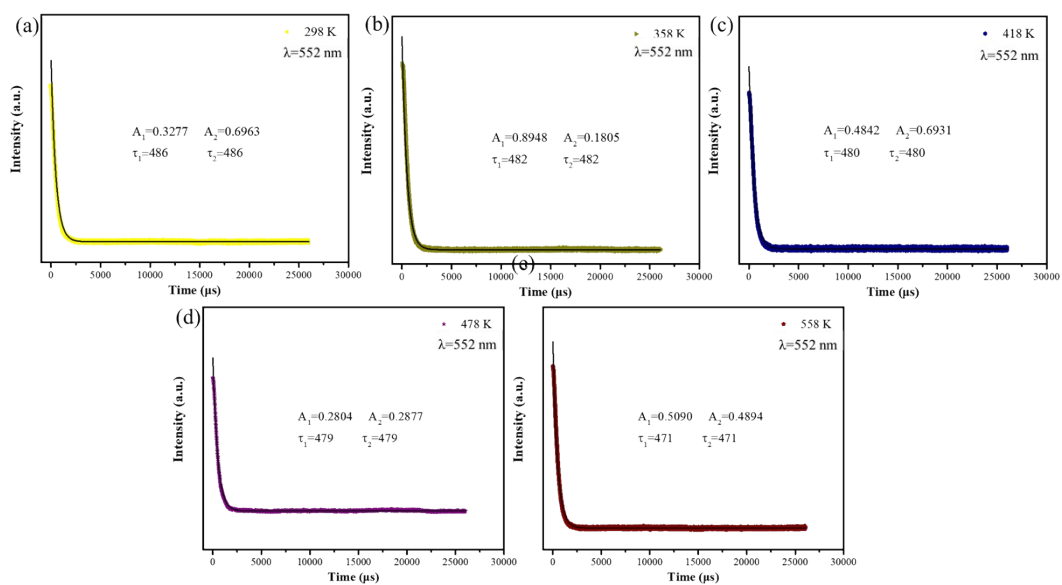


**Fig. S10.** Decay curves of Yb/Er/ZnGdO particles with citric acid content 12 mM of Er<sup>3+</sup> emissions at wavelengths 552 nm under 980 nm excitation at different temperature.

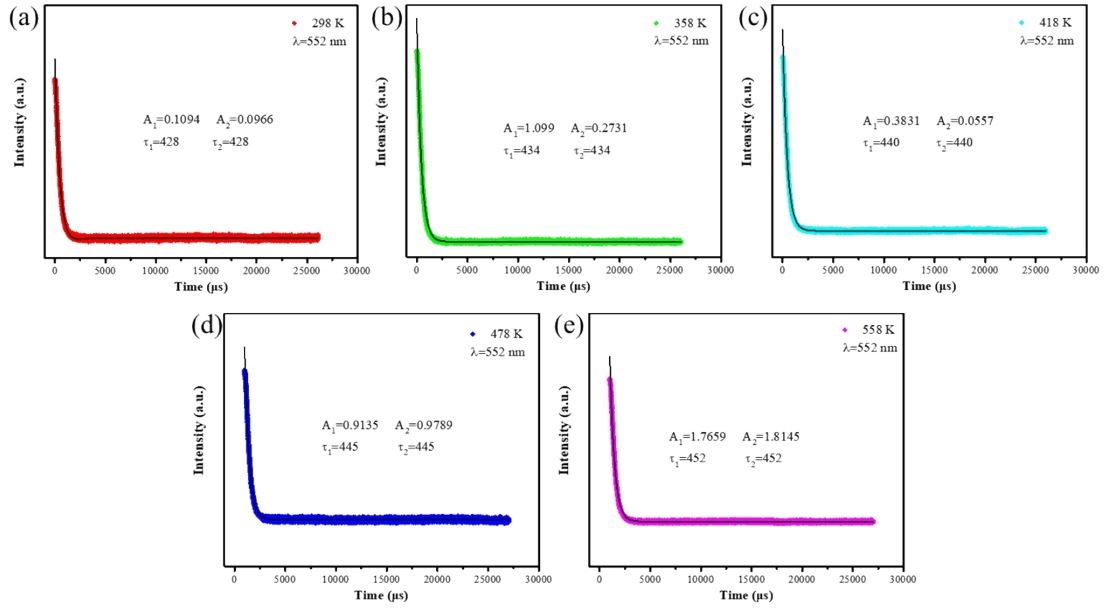


**Fig. S11.** Decay curves of Yb/Er/ZnGdO particles with citric acid content 12 mM of Er<sup>3+</sup> emissions at wavelengths 520 nm under 980 nm excitation at different temperature.

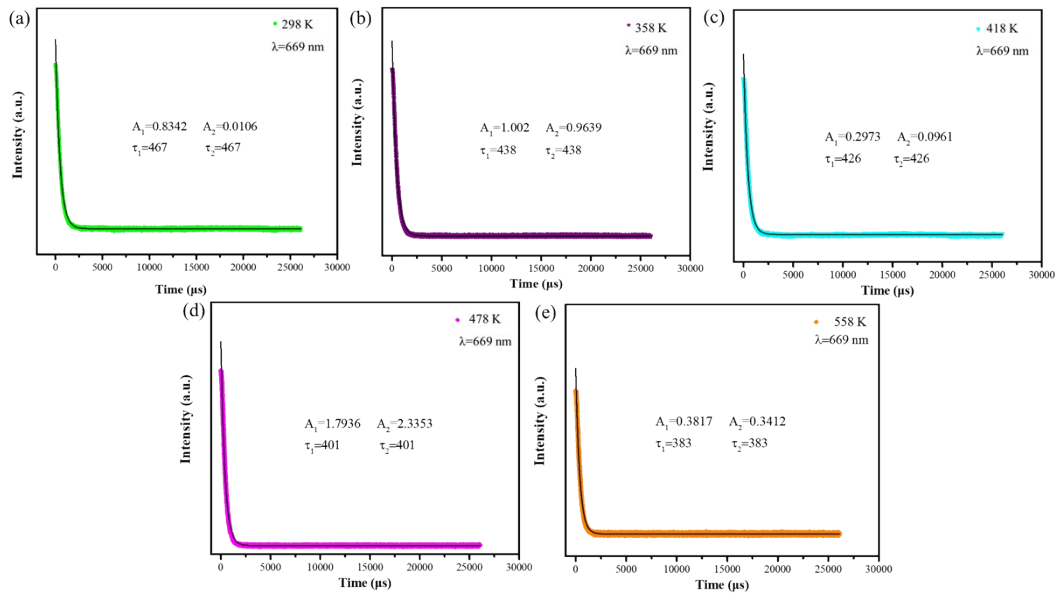


**Fig. S12.** Decay curves of Yb/Er/ZnGdO particles with citric acid content 12 mM of Er<sup>3+</sup> emissions at wavelengths 669 nm under 980 nm excitation at different temperature.

Table S2 Decay curves of Yb/Er/ZnGdO particles with citric acid content 12 mM of Er<sup>3+</sup> emissions at wavelengths 520 nm, 552 nm and 669 nm under 980 nm excitation at different temperature.

Temperature	Lifetime ( $\mu$ s)	lifetime( $\mu$ s)	lifetime( $\mu$ s)
	552 nm	550 nm	669 nm
298 K	486	428	467
358 K	482	434	438
418 K	480	440	426
478 K	479	445	401
558 K	471	452	383